Taylor Vortices in Wide Spherical Shells

M. Liu, C. Blohm, C. Egbers, P. Wulf, and H. J. Rath

Center of Applied Space Technology and Microgravity (ZARM), University of Bremen, Am Fallturm, D-28359 Bremen, Germany

(Received 27 November 1995)

It was believed that no Taylor vortices would exist in wide spherical shells with an aspect ratio of $\beta > 0.24$. In contrast, we have experimentally generated Taylor vortices in a relatively wide spherical shell with $\beta = 0.33$ using some special initial conditions. It is found that the Taylor vortices remain very stable in a range of the Reynolds number $467 < \mathrm{Re} < 2100$, once they are established, in which, normally, the axisymmetric basic state (spherical Couette flow) is preferred. Furthermore, it is interesting that with increasing Reynolds number the Taylor vortices become asymmetric with respect to the equatorial plane. [S0031-9007(96)00599-6]

PACS numbers: 47.32.Cc

The flow in spherical shells is an important problem in fluid dynamics and geophysics. Besides some engineering applications [1], this simple system represents a parade example for study of structure formation [2]. Furthermore, spherical flow is often used to investigate dynamics of large-scale geophysical and astrophysical motions in planetary interior and atmospheres [3]. In this respect, a wide spherical shell seems generally more relevant as, e.g., the whole mantle thickness of the major terrestrial planets (Earth, Venus, and Mars) is believed to be about half of the outer radius.

Geometrically, a spherical shell can be considered as a combination of two other simpler systems with parallel disks in the pole regime and cylindrical annulus near the equator. This is especially the case for narrow shells. Thus in a narrow spherical shell, as in a cylindrical annulus, Taylor vortices can be generated in the equatorial region by rotating the inner sphere above a critical value while the outer sphere is held at rest. These axisymmetric toroidal vortices are driven by the centrifugal force. As the shell width becomes larger the interaction of the two local effects becomes dominant. The strong Ekman pumping at the poles similar to that between two disks alters the flow behavior near the equator. According to the previous experimental observation the spherical geometry regarding the aspect ratio $\beta = d/R_i$ ($d = R_o - R_i$, where R_i and R_o are the radii of the inner and outer spheres, respectively) was divided in three characteristic regimes [4]: the narrow gap with $\beta < 0.12$, the medium gap with $0.12 \leq \beta \leq 0.24$, and the wide gap with $\beta > 0.24$. In narrow and medium gaps Taylor vortices occur as the first instability (the difference between narrow and medium gaps consists of the different torque behavior of the Taylor vortex flow). Since the pioneering work of Sawatzki and Zierep [5], the majority of previous studies on the spherical shell flow concentrated on the medium gap [4,6–9]. In contrast, little attention has been paid to the wide-gap case, where no Taylor vortices could be observed experimentally, as yet. The flow undergoes directly to three-dimensional secondary waves as the first instability [10,11].

Contrary to the above definition, we report here an experimental observation of Taylor vortices in a relatively wide gap with $\beta = 0.33$. The motivation for the present study is given by the existing discrepancy between experimental and theoretical work on describing the flow in this regime. The linear stability analysis with the basic flow presented in a series approximation of Legendre polynomials [12] predicts several critical Reynolds numbers, which are far below the critical onset of three-dimensional secondary azimuthal waves observed in experiments. Moreover, using a continuation method, Schrauf [9] has found numerically that the widest gap in which the flow with one pair of Taylor vortices exists is $\beta \approx 0.45$–0.48 depending on the Reynolds number. His results were, however, argued because a steady-state solver was used and, therefore, the solutions are not necessarily stable [4]. On the other hand, we know that the (spherical) Couette flow is a classical example of nonuniqueness [5]. The final state of the flow depends not only on the Reynolds number and the gap size, but also on the history of the flow. The classification for the wide gap ($\beta > 0.24$) of Marcus and Tuckerman [4] is based on the fact that Taylor vortices have not been generated in the usual way, i.e., by rotating the inner sphere while the outer sphere is at rest. Using this initial condition, the limit for the existence of Taylor vortex was verified and slightly extended to $\beta = 0.25$ by Egbers and Rath [11]. It is imaginable that other basins of attraction in the phase space could be reached if the initial conditions are strongly altered by rotating the outer sphere additionally. In fact, in a work of Belyaev *et al.* [13], which is written in Russian and seems unknown to Marcus and Tuckerman [4], Taylor vortices were also generated in the gap of $\beta = 0.3038$ with the help of the additional rotation of the outer sphere at the beginning. It was said that the generation is very difficult, but without going into any details. However, the situation was, compared to Belyaev *et al.*, more challenging to us because Dumas [14] defined a criterion $\beta < 0.3$ for the mere possibility of developing ultimately Taylor vortices in the spherical Couette flow according to the length-scale analysis. By examining the position of the local maximum in the meridional stream

 0031-9007/96/77(2)/286(4)$10.00

function of the basic flow, he found that for $\beta > 0.3$ there is simply no space available to allow for the formation process to occur (pinched flow, Taylor vortices).

The experimental apparatus used has been described in detail elsewhere [11]. Several sets of the spherical shells are available. For the present study, $\beta = 0.33$ is chosen. The outer sphere ($R_o = 40.00 \pm 0.02$ mm) is made out of transparent acrylic plastic, and the inner sphere ($R_i = 29.95 \pm 0.03$ mm) of aluminum alloy. Generally, both spheres can be rotated independently by means of two belt drives. A silicone oil (Baysilone M3) is used as working fluid. The temperature of the fluid is measured by five temperature sensors (PT 1000) installed on both spheres (two on the inner sphere and three on the outer sphere). The Reynolds number is defined with respect to the inner sphere rotation as $\mathrm{Re} = (2\pi n_i/60)R_i^2/\nu$, where n_i is the rotation rate of the inner sphere per minute (rpm), and ν is the kinematic viscosity of the fluid.

Small aluminum flakes (0.05% by weight) are suspended for visualization. The flow structure is observed through the outer sphere in the area up to the colatitude $\theta = 110°$ (i.e., the northern hemisphere and the equatorial region). A system with a fiber optic is applied to illuminate the global flow structure, while the flow pattern in the meridional cross section of the spherical annulus is additionally visualized by a light sheet technique.

In medium gaps various flow states could be generated by different acceleration rates of the inner sphere from rest to a given Reynolds number, whereas the outer sphere remains always at rest [6]. Our search for Taylor vortices in $\beta = 0.33$ failed in this way. After many experiments with very different combinations of ways allowable by our experimental apparatus, the Taylor vortices could finally be generated by first counterrotating the outer sphere and then stepwise reducing its angular velocity to zero, as illustrated in Fig. 1. In particular, the generating procedure begins with the inner sphere rotating at a constant rate $n_i = 15$ rpm and the outer sphere at $n_o = -10$ rpm (in counter direction of the inner sphere). In this stage the flow is axisymmetric, and the vortex near the outer sphere due to rotation of the outer sphere dominates, as sketched in Fig. 1(a). After a few minutes, the frequency of rotation of the outer sphere is reduced to $n_o = -6$ rpm. The flow becomes three dimensional; a single spiral, as sketched in Fig. 1(b), travels azimuthally following the outer sphere rotation. The traveling speed decreases very slowly in time. After another few minutes, the outer sphere is stopped and one pair of Taylor vortices occurs, which is axially and equatorially symmetric, as shown in Fig. 2(a). With this procedure, which will be referred to as "step method," we succeeded in generating Taylor vortices by about 20%. The time elapsed in the second stage ($n_o = -6$ rpm) is decisive and it should be about 3 min. In this way Taylor vortices can be generated only by holding the inner sphere rotation in the range of $494 \leq \mathrm{Re} \leq 526$. Later, we found that Taylor vortices could be induced more easily and quickly, although not always, by a small tick of outer sphere in the counter direction with hand, whereby the inner sphere is held at $\mathrm{Re} = (525 \pm 5)\%$.

Figure 3 shows the evolution of the flow as the Reynolds number is changed in terms of the modes observed. We see that the basic state (spherical Couette flow) is always stable before the first instability in the form of the secondary waves occurs at about $\mathrm{Re} = 2800$. Taylor vortices coexist in the range of about $470 \leq \mathrm{Re} \leq 2100$ and merge into the basic flow state at both Re limits. We note that the Taylor vortices are rather stable against small disturbances, once they are generated. With the constant acceleration time of 10 sec (in which the Reynolds number is increased linearly from one to the other), no premature transition to the basic flow occurred by the maximum applied step size of $\Delta\mathrm{Re} \approx 160$. At $\mathrm{Re} \approx 1600$ Taylor vortices become wavy and the amplitude of about four to six azimuthal waves grows with increasing Reynolds number until the vortices are finally destroyed abruptly. It is unclear if

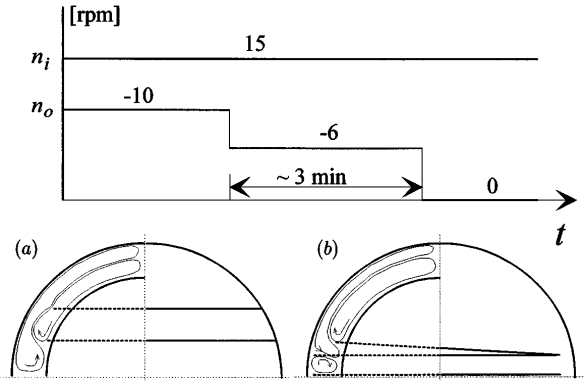

FIG. 1. Upper: Generation procedure of Taylor vortices. Lower: Two typical flow configurations in the transient stage at (a) $n_o = -10$ rpm and (b) -6 rpm.

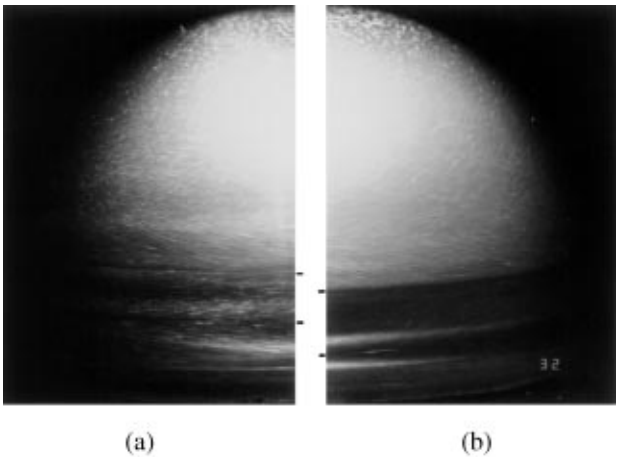

FIG. 2. Experimental photographs of the Taylor vortex in the northern hemisphere: (a) Equatorially symmetric mode at $\mathrm{Re} = 535$; (b) equatorially asymmetric mode at $\mathrm{Re} = 1840$. The location of the vortex is additionally depicted by bars at the vortex boundary.

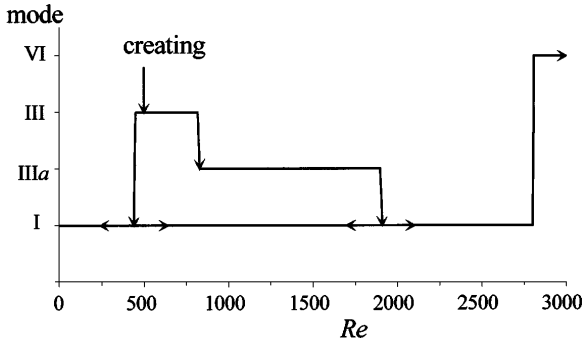

FIG. 3. Flow modes in $\beta = 0.33$. Mode I: spherical Couette flow; mode III: axially and equatorially symmetric Taylor vortices; mode IIIa: axially symmetric but equatorially asymmetric Taylor vortices; mode VI: three-dimensional secondary waves.

the wave motion is induced by geometrical imperfection of the apparatus such as the supporting shaft of the inner sphere located at the south pole.

In the course of experiments, a further interesting phenomenon was observed: The Taylor vortices become asymmetric with respect to the equatorial plane as the Reynolds number is increased to about Re = 650, as shown in Fig. 2(b) for Re = 1840. This effect has been observed by Bühler [8] both experimentally and numerically for the gap of $\beta = 0.154$, but not yet in other medium gaps. In order to investigate if the magnitude of the asymmetry and its onset depend on the step size of Re enhancement (ΔRe), many runs with different ΔRe ($\Delta n_i = 0.25{-}5$) were carried out. The waiting time at each step is at least 3 min (the viscous diffusion time from the inner to outer sphere is about 30 sec, and from the pole to the equator is about 12 min). The relative width (s/d) of the Taylor vortex in the northern hemisphere and its displacement ($\Delta s/d$) from the equatorial plane with respect to the gap width are shown as a function of the Reynolds number by different increasing rates of Re in Fig. 4. The measurement was done on the monitor of the video records (no optical correction is performed because it is not essential in this case). It is interesting to note that Taylor vortices are always displaced in the southern direction ($\Delta s/d < 0$) when they are generated by the step method. If Taylor vortices are generated manually, a displacement in both directions was observed. A rough estimate appears that the asymmetry goes northward when Taylor vortices are generated by Re > 525, and southward by Re < 515, although no difference in the Taylor vortices at this low Re regime could be recognized. In one case we also observed a sign change of the displacement first in the northern and then in the southern direction as the Reynolds number was increased.

From Fig. 4, no significant dependence of the vortex width and the asymmetry on the step size of Re enhancement can be recognized. The width of the Taylor vortex grows quickly with the Reynolds number up to about

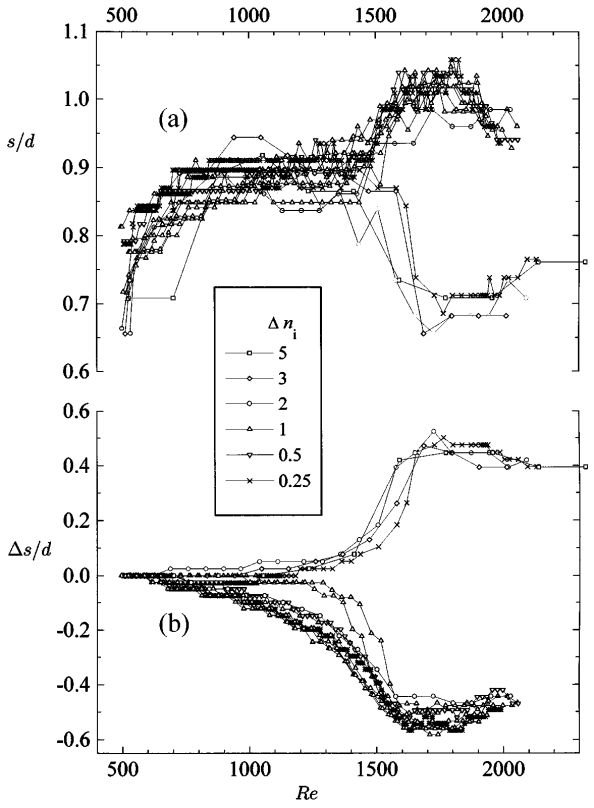

FIG. 4. Characteristics of asymmetric Taylor vortices at high Reynolds numbers. Several runs have been carried out for $\Delta n_i = 1$. See text for explanation.

Re = 750, and then remains essentially constant up to about Re = 1400. Increasing the Reynolds number further, a wholly different development in the vortex size takes place. Comparing to the displacement in Fig. 4(b) we see that a further growth of the vortex occurs when the vortex is displaced in the southern hemisphere; in contrast, the vortex size decreases when it is displaced in the northern hemisphere. The asymmetry appears in most cases already at Re $\approx$ 650, but in some cases at Re $\approx$ 1100 first. By reflecting the upper (positive) curves in Fig. 4(b) downward, it can be seen that the bifurcation follows essentially two loops. For the step size ΔRe = 1 several runs are performed and it seems random, in which loop it falls.

After generating Taylor vortices in $\beta = 0.33$ experimentally, we have tried to simulate them numerically with the initial-value finite-difference code of Liu, Delgado, and Rath [15]. This code was, however, developed only for axially symmetric flows in the spherical shell. The reconstruction with the conditions as in the step method did not succeed in obtaining Taylor vortices, presumably due to the three-dimensional nature of the flow in the second stage [the axisymmetric flow structure as in Fig. 1(a) could be simulated directly]. However, with wholly different combinations of the inner and the outer sphere rotation as well as the duration at each step, through trial and

error, we have actually generated a pair of Taylor vortices in $\beta = 0.33$ directly from the rest initial state.

With the initial-value code of Liu *et al.* [15] we also studied the existence of the Taylor vortices in the (Re, β) plane, because a steady-state solver was used by Schrauf [9] and the solution is therefore not necessarily stable [4]. Our results as well as Schrauf's are shown in Fig. 5. The agreement of two curves is apparent except in the upper right regime. Our curve with a higher resolution of 25×120 grid points lies generally within the Schrauf's (21×121). This is consistent with the estimate of Schrauf that the higher resolution shifts the curve inward. From our calculations the widest gap in which Taylor vortices remain stable is $\beta = 0.483$ (by $\mathrm{Re} = 1400$). Compared to our experiments, we note that the numerical value of the lower Re limit of Taylor vortices existence for $\beta = 0.33$ is about 50 smaller than the experiment. Moreover, we found that, in contrast to the experiment, Taylor vortices by the numerical simulation (of course, no equatorial symmetry is imposed numerically) always remain symmetric with respect to the equatorial plane in the whole Re range studied. This may be relevant to the result of Bühler [8] for $\beta = 0.154$, where the equatorially asymmetric mode could be simulated numerically only with the very special initial conditions not identical to the experiments.

We have also tried to generate Taylor vortices in the presently available next wider spherical shell with $\beta = 0.5$. No stable Taylor vortices could be established, although they have often been observed at the initial phase after manually rotating the outer sphere. This may confirm the numerical results.

The linear stability analysis in [12] for the only (very wide) spherical shell of $\beta = 1$ shows a critical Reynolds number at 325. We note that this value is extrapolated because for $\mathrm{Re} > 225$ numerical difficulties were encountered in the integration of the system of nonlinear ordinary differential equations governing the basic flow. It is therefore unclear if this mode corresponds to the Taylor vortices. However, it was found that the critical mode was nonsymmetric with respect to the equator, which may be consistent with the asymmetric behavior of Taylor vortices at high Reynolds numbers found in our experiments.

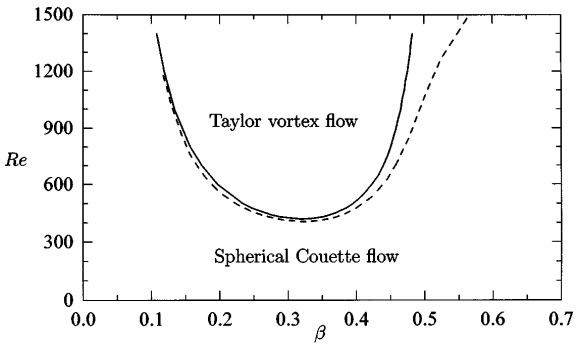

FIG. 5. Existence regime of the Taylor vortices based on the numerical simulation. Dashed line is results of Schrauf [9].

In summary, we have, for the first time, found and studied stable Taylor vortices in a wide spherical shell $\beta = 0.33$ experimentally. This study partly verifies the numerical calculations of Schrauf [9]. A further novel feature of Taylor vortices from this study is that the vortices become asymmetric with respect to the equator at high Reynolds numbers. Clearly, many additional experiments are required in order to understand the phenomena revealed in this study, for example, why the Taylor vortices become equatorially asymmetric at high Reynolds numbers, and why the Taylor vortices merge into the basic state instead of persisting to higher Reynolds number until the first instability in the form of the secondary waves occurs. Furthermore, we need a more precise apparatus with better controlled temperature and rotation rate in order to quantify the initial conditions and the behavior of the asymmetry.

This work was supported by the Deutsche Agentur für Raumfahrtangelegenheiten (DARA) and the Senator für Bildung, Wissenschaft und Kunst des Landes Bremen.

[1] K. Bühler, in *Strömungsmechanische Instabilitäten zäher Medien im Kugelspalt*, Fortschritt-Berichte VDI, Reihe 7, Stromungstechnik, Nr. 96 (VDI Verlag, Düsseldorf, 1985).
[2] M. Wimmer, Prog. Aerosp. Sci. **25**, 43 (1988).
[3] K. G. Roesner, in *Proceedings of the International Conference on Numerical Methods in Fluid Dynamics* (Springer-Verlag, Berlin, 1978).
[4] P. S. Marcus and L. S. Tuckerman, J. Fluid Mech. **185**, 1 (1987).
[5] O. Sawatzki and J. Zierep, Acta Mech. **9**, 13 (1970).
[6] M. Wimmer, J. Fluid Mech. **78**, 317 (1976); **103**, 117 (1981).
[7] F. Bartels, J. Fluid Mech. **119**, 1 (1982).
[8] K. Bühler, Acta Mech. **81**, 3 (1990).
[9] G. Schrauf, J. Fluid Mech. **166**, 287 (1986).
[10] I. M. Yavorskaya, Yu. N. Belyaev, and A. A. Monakov, Fluid Mech. **5**, 660 (1975).
[11] C. Egbers and H. J. Rath, Acta Mech. **111**, 125 (1995).
[12] B. R. Munson and M. Menguturk, J. Fluid Mech. **69**, 705 (1975).
[13] Yu. N. Belyaev, A. A. Monakhov, G. N. Khlebutin, and I. M. Yavorskaya, Space Research Institute, USSR, Academy of Sciences, Moscow, Report No. 567, 1980.
[14] G. Dumas, thesis, California Institute of Technology, 1991.
[15] M. Liu, A. Delgado, and H. J. Rath, Comput. Mech. **15**, 45 (1994).